# Trends in Deep Learning for Medical Hyperspectral Image Analysis

**UZAIR KHAN**[1], **SIDIKE PAHEDING**[2], **COLIN P. ELKIN**[1], (Member, IEEE), AND **VIJAYA KUMAR DEVABHAKTUNI**[1], (Senior Member, IEEE)

[1]Department of Electrical and Computer Engineering, Purdue University Northwest, Hammond, IN 46323, USA
[2]Department of Applied Computing, Michigan Technological University, Houghton, MI 49931, USA

Corresponding author: Sidike Paheding (spaheding@mtu.edu)

**ABSTRACT** Deep learning algorithms have seen acute growth of interest in their applications throughout several fields of interest in the last decade, with medical hyperspectral imaging being a particularly promising domain. So far, to the best of our knowledge, there is no review paper that discusses the implementation of deep learning for medical hyperspectral imaging, which is what this work aims to accomplish by examining publications that currently utilize deep learning to perform effective analysis of medical hyperspectral imagery. This paper discusses deep learning concepts that are relevant and applicable to medical hyperspectral imaging analysis, several of which have been implemented since the boom in deep learning. This will comprise of reviewing the use of deep learning for classification, segmentation, and detection in order to investigate the analysis of medical hyperspectral imaging. Lastly, we discuss the current and future challenges pertaining to this discipline and the possible efforts to overcome such trials.

**INDEX TERMS** Deep learning, neural networks, machine learning, medical image analysis, medical hyperspectral imaging.

## I. INTRODUCTION

Medical imaging refers to images used to aid in clinical work relative to the human body such as surgical procedures, diagnoses for impeding diseases, or simply to analyze and study body functions and is primarily based on radiological research. For the last couple of decades in particular, modern imaging techniques such as X-rays, magnetic resonance imaging (MRI), and ultrasound have had significant impacts on not only medical symptoms analysis but also on the spawning of more imaging techniques for improvised examination. Computed tomography (CT) scan, for example, is an X-ray procedure that displays the cross-sectional image of the body, which now also helps to assess brain or head-related injuries [1]. Another circumstance in which X-rays have been influential for further progress in research and application is mammography, in which a low energy x-ray photon beam is implemented to diagnose breast cancer, which is presently a common medical problem worldwide [2]. These implementations of X-rays are part of practices known as computer-aided diagnosis (CAD), which is a methodology used to assist clinical procedure to perform diagnosis [3]. More than often

The associate editor coordinating the review of this manuscript and approving it for publication was Essam A. Rashed.

for medical imaging, image fusion is utilized, in which the final output image consists of more meaningful information and is obtained from multiple input images [4]. An emerging imaging method in the discipline of biomedicine is Terahertz (THz) imaging, which is currently working to overcome its limitations with the aid of nanotechnology by finding its roots in the highly promising medical imaging methodology and becoming safer than traditional methodologies [5]. The primary goals for any effort to obtain medical images for diagnosis is via a non-invasive and inexpensive methodology.

Hyperspectral imaging (HSI) is a developing imaging technique amid the medical imaging modality and offers a noninvasive disease diagnosis in majority of cases. HSI comprises of various images aligned in adjacent narrow wavelengths or spectral bands (often in the range of hundreds) and recreates a reflectance spectrum of all the pixels in the band [6]. This is done by separating light using a spectral separator consisting of bandpass filter(s) and accumulating it on a focal plane detector (typically a complementary metal oxide semiconductor (CMOS) sensor) to form the image. This provides a method to perform medical image diagnosis which is relatively safer when radiation is considered, provides real-time images, and also provides a greater bandwidth resolution with which to perform diagnosis [7].

Hyperspectral imaging has traditionally been used for remote sensing [8], [9], agriculture [10], food safety & quality assessment [11], [12], image enhancement [13], disaster monitoring [14], [15], feature extraction [16], classification [17], object detection [18]–[20], and recently even for conservation of art [21]. For medical imaging, it is principally obtained by targeting tissue samples by transmission of light and used to diagnose and detect various types of cancers [7] and other medical applications. With cancer being the second leading cause of death in the US, this significantly impacts the medical society and its research to eliminate cancer. Medical Hyperspectral Imaging (MHSI) has previously aided in successfully distinguishing between tumors and normal tissues from a rat breast tumor model, providing a clear indication of how influential MHSI can be for future research on breast cancer [22]. It has also proven its significance in detection of cancerous tissue cell detection from normal tissue specimen for neck and head cancer [23]. Gastric cancer is one of the leading causes of cancer-related deaths in the world, and its future diagnosis will also be significantly simplified thanks to MHSI [24]. All these MHSI applications for several medical diagnoses have led to the development of multiple algorithms to more accurately and efficiently classify the cancerous tissues from a sample [25], which further instigates on the different techniques for the processing and analysis of MHSI.

Artificial Intelligence, and its most common subset known as Machine Learning (ML), is a highly popular approach to process hyperspectral images and extract meaningful data from it. ML algorithms make use of data and statistical models to learn and identify patterns to complete specific tasks and make decisions with or without human supervision. Several such ML algorithms are utilized when examination of hyperspectral images is considered and consequently in identifying and classifying differences in a tissue specimen when studying MHSI. While ML algorithms can be rudimentarily divided into supervised and unsupervised learning models, the algorithms are prone to develop into increasingly complex models as we delve further into Deep Learning (DL) [26], a branch of ML that is influenced by the structure and function of the human brain. In supervised learning, the model is fashioned from a dataset containing a number of input features and outputs, or labels. This model is formed by finding the optimal model parameters from a training sample of the dataset, which is subsequently used to predict the outcome based on the minimized cost function. Unsupervised learning processes data without any particular structure and is trained to find patterns and typically create groupings based on clusters.

Traditional ML algorithms typically used for MHSI applications lean towards classification models for identification and diagnosis, which also includes $k$-nearest neighbors (kNN) [27], linear discriminant analysis (LDA) [28], and support vector machines (SVM) [29]–[31], with the latter being the most prominently applied. With ML already heavily facilitating the processing of MHSI, the next logical step is to apply deep learning to achieve a more cost-effective and more accurate prediction model, thereby providing a more comprehensive diagnosis to this pertaining medical issue. Deep learning in general has started taking off extraordinarily as early as 2012 [32], [33], and deep learning for MHSI has been no different in this regard. This subset of ML has already proven to outperform traditional ML techniques in the principle of head and neck surgery [34] and looks promising for MHSI in a broader aspect. Deep learning has also been applied for classification of a previously listed example related to head and neck cancer and shows significant improvement in accuracy over SVM and kNN [35].

Our end goal from this paper will be to highlight the key DL methods being used for MHSI and the challenges for successful application of DL in MHSI. This is because the DL methods to be implemented for MHSI in the coming decade will have a significant implication for future studies in several key areas of the medical discipline, including cancer research. The rest of the survey will be discussed as follows: Section 2 will introduce the fundamentals of DL methods that are currently being used as well as several emerging algorithms. Section 3 will discuss which DL methods are presently implemented for MHSI as well as additional algorithms that could be applied in the coming decade. Section 4 will ultimately discuss the current challenges faced by DL for MHSI.

As previously mentioned, the trend in research for DL methods being used for MHSI has seen a sudden surge since as recently as 2012. This can easily be traced back to the ImageNet Large Scale Visual Recognition Challenge (ILSVRC) that was conducted in 2012, in which a deep learning method, which we will discuss later in Section 2, broke prior records by providing accuracy results close to 41% better than the best previous attempt [36]. Since then, more and more researchers have explored DL methodologies in a wide array of disciplines. Our survey covers papers published that specifically target the confrontation of medical hyperspectral imaging with deep learning techniques. For papers to be considered valid for our purpose, we examined keywords and selected the papers from only major publishers comprising of IEEE, Elsevier, Springer, SPIE, MDPI, International Journal of Biomedical Imaging, Journal of Biomedical Optics, and a handful of small publishers in some scenarios via Google Scholar as well as the publisher's respective search engines, with the latest being published in December 2020. While numerous publications are already present for deep learning being implemented for medical image analysis, with our topic of discussion being so highly specific, we cross-checked all sections within the publications that matched the subject matter of deep learning being implemented for medical hyperspectral imaging to verify papers for this survey. For certain situations in which published work corresponded with multiple papers, we only considered papers with greater significance in regard to their contributions. The goal for these papers being included in this survey, as mentioned earlier, encompassed the benefits of deep learning methodologies, how they are contributing towards medical hyperspectral imaging, and the challenges

being faced for effectively applying these deep learning techniques to medical hyperspectral imaging. Fig. 1 provides a summary of the number of most relevant papers published throughout the specified range of years.
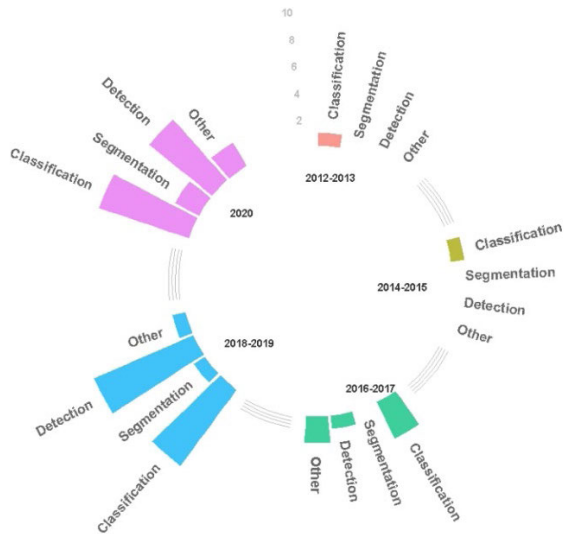


**FIGURE 1. Chart representing the number of relevant papers published in the past years. The bars depict the quantity of papers published spread apart evenly for every two consecutive years for each category of DL methodology.**

## II. DEEP LEARNING METHODS

Machine Learning methodologies are typically divided into either supervised or unsupervised learning algorithms. A learning algorithm that makes use of a dataset comprising of a set of input features and an output label to obtain a predicting model is known as a supervised learning algorithm. The output label in the dataset for supervised learning can be categorized as either classification or regression. A classification problem categorizes the output into discrete values such as type A and type B. A regression problem provides the output as a continuous value, which could represent a real value such as dollars or a more symbolic numerical value, such as a normalization of a different number. The learning part in supervised learning refers to finding the optimal weights or parameters that minimize the cost (or loss) function. This would mean that no further loss can be achieved and that the weights cannot be further improvised, which results in the best-fit model with the given inputs, bias, and learning rate. After successfully creating the model, a portion of the data is used to test the accuracy and/or the efficiency of the model. This is simply done by comparing the output from the model against the actual value from the dataset. While this is also implemented in the process of minimizing the cost function, the goal of testing the model is to perceive the vulnerability of the model.

An unsupervised learning algorithm is used to figure out the underlying structure of a dataset, which does not consist of a definite output. The algorithm does this by either clustering the output into categories or by finding the associative properties among the input parameters. Since the initial weights

and parameters are selected ambiguously, the resulting output is not always similar every time, as a different model is obtained during every training process. In the following sections, we will delve upon various deep learning methods, which are built upon the aforementioned-ML fundamentals.

### A. SUPERVISED LEARNING METHODS

#### 1) NEURAL NETWORKS

Neural Networks are a category of learning algorithms built upon the idea and structure of a human brain, as the name suggests, and it lays the foundation for the majority of the deep learning methods. A neural network contains layers of neurons (known as a perceptron) as the base unit, which comprises of an activation number and other sets of parameters, such as weights W and bias b. This can be simplified to an activation function, which can be expressed as

$$a^{(1)} = \sigma(Wa^{(0)} + b), \qquad (1)$$

where $a^{(0)}$ represents the initial activation numbers, or the input features, and $a^{(1)}$ refers to the activation numbers for the next layer. The $\sigma$ refers to the transfer function, which is traditionally denoted as either a sigmoid function or a step function. To form a fully constructed layer at each interval, we obtain the dot product between the weight vector and the input features vector. This represents a single layer of neurons, which has a simple feedforward mechanism, i.e. the neuron takes in a single input, performs the operation on it, and then passes it on to the next layer. A multi-layer perceptron (MLP) consists of two or more layers of neurons or perceptrons, which are also known as hidden layers. All of these layers from MLP combine together to form the basis of what is more commonly known as a Deep Neural Network (DNN). While there are different additional DNN techniques, on which we will be expanding next, MLP is one of the most basic DNN architectures. Fig. 2 (a) and (b) depict simple and deep neural network architectures, respectively.
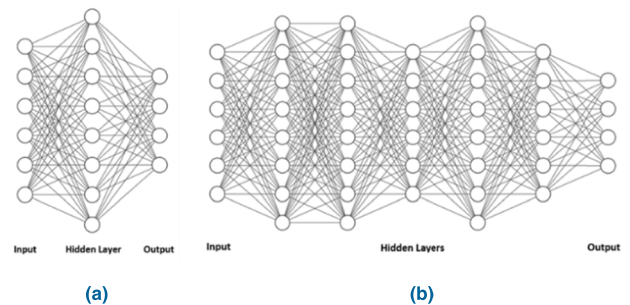


**(a)** **(b)**

**FIGURE 2. Visual representation of (a) simple neural network: a machine learning algorithm modeled from the biological neural network of a human brain, (b) deep neural network: a neural network comprising of more than one hidden layer of neurons for its architecture.**

#### 2) CONVOLUTIONAL NEURAL NETWORKS

Convolution Neural Network (CNN) is an exceedingly popular deep learning algorithm that is used to classify an input image by recognizing patterns and features in order to differentiate between objects. In fact, one of the earliest perceptron
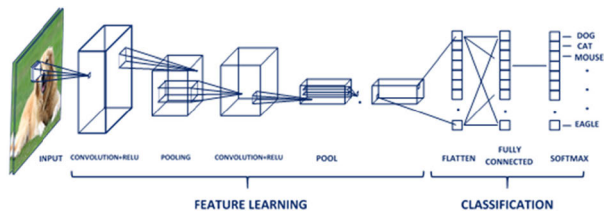
**FIGURE 3.** Convolutional Neural Network (CNN): a deep learning architecture containing several convolutional and pooling layers, which are then connected at the output. This output in turn is used to classify the input image provided. CNN has proven to be exceeding popular in computer vision and visual image analysis as of late due to its high accuracy and precision.

concepts in 1957 was designed with the purpose of classifying the input image as man or woman [37]. The weights in a CNN architecture are designed to perform convolution operations on the input image rather than the features. In a convolution layer, the spatial structure is preserved along with any temporal dependencies with the usage of filters or kernels. This means that instead of appropriating a weight for an input feature via the combined stretched matrix from the input features, a small filter with appropriate dimensions relative to the input image is applied to perform the element-wise dot product between the filter and a chunk of the image otherwise 'convolved' in order to obtain the activation. Note that the depth of the filter should match the depth of the image to make this convolution possible. This process is repeated over all the spatial locations of the image, thereby providing us with a final activation map over the spatial region. Fig. 3 represents the overall process of a CNN and how the final output is obtained.

CNNs are a predominant part of typical classification architectures widely used in medical image analysis. One example for simpler architectures would be LeNet [38], which was introduced over two decades ago, which despite being a rather shallow network, displayed the basic concept of a CNN in a simple and elegant fashion, using the tangent function as the activation function. Later on, AlexNet [36] shattered expectations at the ILSVRC in 2012. Bearing similar characteristics to LeNet, AlexNet [36] also made use of kernels with a larger field of layers closer to the input and smaller kernels closer to the output, with the key difference being in the assimilation of rectified linear units (ReLU) for the activation function, which has since become the activation function of choice for modern CNNs due to higher classification accuracy. It can be duly noted that the rise in popularity of deep learning techniques also coincides after this series of events.

### 3) U-net

Segmentation is a popular architecture not only among the medical image analysis community but also for the field of computer vision in general. While CNNs classify the pixels of an image, segmentation provides inference by making prediction labels for each pixel that facilitates the enclosing of core object locations, thus separating the image into sections

of fields. While this provides the unfortunate overlap of neighboring pixels over regions with the same convolutions being computed multiple times, several solutions have been proposed to overcome this ordeal, the most prominent of which is known as a Fully Convolution Network (FCN). The core idea behind FCN is to take the original CNN with arbitrarily sized input images and use the fully connected layer as convolutions to produce the segmented output. However, this still results in a degraded feature map due to the propagation through several pooling layers.

U-net architecture [39] provides a solution for this issue built upon the foundation of the FCN. This architecture consists of the basic FCN supported by an upsampling layer as opposed to a pooling layer, which concludes in an increase in resolution for the final output image. It uses stochastic gradient descent to train the network and calculate the energy equation with the aid of SoftMax, implemented pixel-wide across the final feature map in which the Softmax layer is defined as

$$p_k(x) = \frac{e^{a_k(x)}}{\sum_{k'=1}^{K} e^{a_k(x)}}, \qquad (2)$$

where $a_k(x)$ is the activation function. This is then applied to an energy equation as

$$E = \sum w(x) \log(p_{k(x)}(x)), \qquad (3)$$

where $w$ is the weight matrix for the model. This energy function is, in short, a combination of the Softmax layer over the final feature map with the cross-entropy loss function. Fig. 4 shows the basic architecture of U-net.
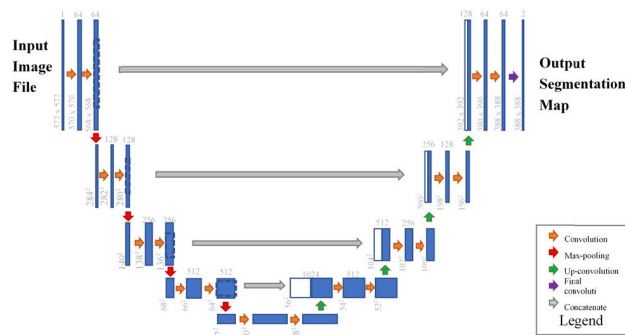


**FIGURE 4.** U-net architecture: a deep learning algorithm based upon Fully Convolutional Network (FCN) that in itself is built upon the foundation of CNN. A majority of the segmentation techniques involve u-net in one way or another, with it forming the core component of a proposed model for segmentation.

### 4) RECURRENT NEURAL NETWORKS

Recurrent Neural Networks (RNNs) were developed with the thought of tackling the progression of vectors over time, which is something CNNs cannot accomplish, as they are restricted to handling fixed vector sizes to provide fixed-size outputs. In addition, CNNs operate on a fixed number of layers. RNNs, by contrast, can have input and output vectors of varying lengths, which make them invaluable for undertaking problems in the Natural Language Processing (NLP)
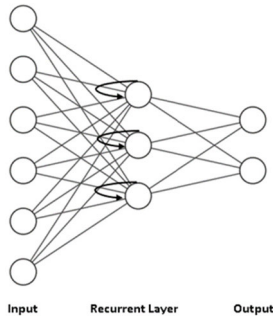
**FIGURE 5.** A simple Recurrent Neural Network (RNN): a neural network in which the previous output is also used as inputs to modify the state of the hidden layer neuron. RNN has the capability of processing inputs of varying lengths without change in the model size, which is invaluable for constantly evolving datasets.

domain [40], as the input matrix in such an application is constantly evolving. Another way in which the RNNs differ from traditional CNNs is that they are not feedforward systems and instead loop the outputs of each hidden layer back to itself. For a classification problem, the output from the hidden layer is used as the inputs along with the normal input for the hidden layer. Fig. 5 shows the comprehensive visual representation of RNN.

### B. UNSUPERVISED LEARNING METHODS

#### 1) AUTO-ENCODERS

Autoencoder is a type of neural network that is primarily trained to provide a learned representation of the input. In other words, an autoencoder generates a replicate for the provided input after undergoing a handful of operations. These operations are performed over a single hidden layer in which the model 'encodes' and then 'decodes' the input to provide the mapped output. Although this process might seem meaningless on the surface, this gives us the opportunity to map how data is projected for a lower dimension. This is because the hidden layer has the smallest dimension in this network, and it also encompasses all the information to reconstruct the output for the same class of input. This is particularly useful in the case of anomaly detection, in which the autoencoder is fed the inputs from the same class of data. Since the mapping features would produce an incoherent result with respect to the autoencoder hidden layer, the anomalies would be discovered easily. Fig. 6 represents the AEN in its rudimentary form.

#### 2) RESTRICTED BOLTZMANN MACHINES

Restricted Boltzmann Machines (RBMs) are a relatively simpler deep learning system comprising of two layers: input and hidden. This forms the basis of deep belief networks. The nodes (neurons) from each layer form inter-layer connections while 'restricting' intra-layer connections, which helps to derive its name. The RBM comprises of bidirectional communications between layers and is thus a generative model that uses the hidden layer to fashion new data points. It does so by defining an energy function for a state of input and visible
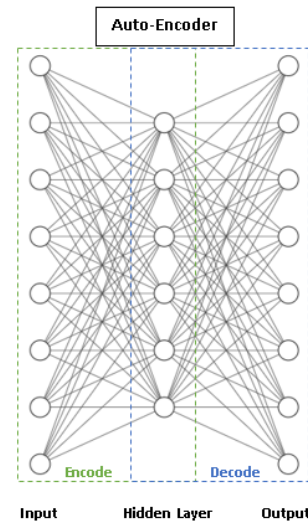


**FIGURE 6.** Comprehensive layout of an autoencoder: a type of neural network that is used to understand the efficient data coding, which is particularly useful for dimension reduction for a given dataset.

units of (y,z) as

$$E\left(y, z\right) = \sum_i a_i y_i - \sum_j b_j z_j - \sum_i \sum_j y_i w_{i,j} z_j, \quad (4)$$

where $a$ and $b$ are the biases, $w$ is the weight matrix, and $y$ and $z$ are the states for hidden unit $j$ and visible unit $i$. The pair of possible hidden and visible vector is computed by finding the probability as

$$p(y, z) = \frac{1}{z} e^{-E(y,z)}, \quad (5)$$

where z is known as a partition function. The RBMs are primarily used to pre-train a NN to generate the initial weights and then are used to form the foundation for other deep learning methods such as a Deep Belief Network (DBN). These DBNs are then used for many different applications, including cybersecurity [41], NLP [42], and of course medical image analysis [43]. Fig. 7 represents a RBM block diagram.

#### 3) GENERATIVE ADVERSARIAL NETWORKS (GANs)

GANs, used widely in image, video, and audio generative scenarios [44], are a generative architecture (as the name suggests) based largely on probability-related setups for unlabeled datasets, which provide a better substitute to maximum likelihood estimators. A GAN architecture pits two neural networks against one another, with the purpose of generating synthetic labels that are comparable to actual data. In each iteration run, the two neural networks keep improving repeatedly at the required task. This procedure continues until the output from the generator resembles the actual sample data as closely as possible.

The generator network and the discriminator network competing against each other, as displayed in Fig. 8, can be considered the two supposed neural networks that highlight the concept of GAN as an example. The example can be
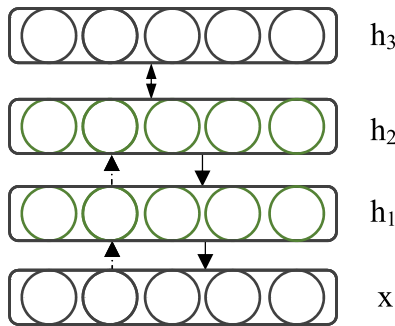
**FIGURE 7.** RBM block diagram: A stochastic neural network that uses bidirectional layers (and consequently generative), comprising of hidden layers (h1, h2, & h3) and input layer x to effectively learn probability distributions for the given set of inputs.
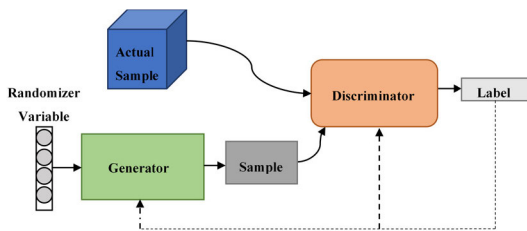


**FIGURE 8.** Generative Adversarial Network block diagram: an architecture that pits two networks against each other, which is used to eventually learn the patterns of the input data in order to produce an output as closely as possible to an actual sample of the input.

considered as a min-max situation, in which the function V (D,G) can be described as

$$min_G max_D V(D, G) = E_{x \sim P_{data}(x)}[\log(D(x))] \\ + E_{z \sim P_{data}(z)}[\log(1-D(G(z)))]. \quad (6)$$

## III. DL METHODS FOR MHSI

### A. CLASSIFICATION

Classification for pathological images has been one of the earliest fields of not just MHSI but medical analysis in general, in which deep learning techniques have been a significant influence. Typical procedures for processing the MHSI using classification include applications such as cell classification [45] in order to identify and classify cancerous cells. This is also sometimes synonymous with detection techniques on the surface, in which the architecture is designed to detect traces of cancer from samples, as opposed to just classifying the cells themselves, which we will discuss in the next section. Classification techniques for MHSI often make use of transfer learning, which has proven to be quite useful in these scenarios. MHSI typically utilize small datasets comprising of medical diagnosis images (typically hundreds or thousands), as opposed to the field of computer vision in which the datasets could consist of millions of sample images, which is one of the reasons why transfer learning has been feasible for this discipline. A generalized process for the classification process for cancerous cells is displayed in Fig. 9.

Transfer learning is fundamentally the use of a pre-trained network to classify input images from testing samples, and
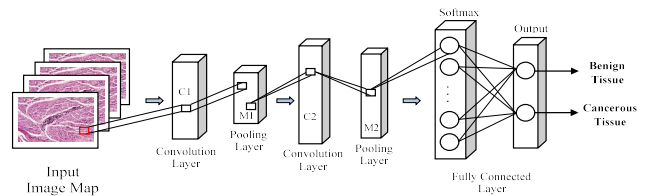


**FIGURE 9.** Visual representation of classification of a cancerous tissue sample.

as mentioned earlier, the smaller datasets allow greater practicality and ease of use, as opposed to training the network to obtain new input features every time for virtually similar input image datasets. The implementation of deep learning for MHSI took some time to catch on when compared to deep learning used in other areas of research. Earlier implementations of deep learning in MHSI began with classification of benign & malignant tissues or cell samples using ANNs, typically MLPs [7]. A particular study that explores HSI for characterizing kidney stones [46] made use of Principal Component Analysis (PCA) to determine appropriate variables or features to be extracted and used for a simple ANN model comprising of a hidden layer with four nodes, which was used to classify the type of kidney stone from the HSI, whereas a similar approach was also undertaken to classify different cancer types [47] [48]. There have been situations in which ANNs provided inferior results, which in turn highlights the problems related to deep learning, namely the absence of larger datasets. This particular study assessed the performance between four supervised algorithms that pitted ANN against random forest, SVM, and k-nearest neighbors [49]. The paper utilized a three-stage framework, with the first stage implementing pre-processing on the input data of oncologic esophageal resectates in order to tackle the class imbalance in the output labels. The second stage of the framework implemented the different classifiers and eventually found that from the 11 patient samples analyzed, SVM produced the best results, although they did remark that a larger training dataset may lead to better performance in general. Another such paper which was utilizing several classifiers as part of the proposed framework found that ANN underperformed when compared to SVM and random forest (RF) [50].

In more recent years, however, CNNs have become the prevalent choice for the task of tissue/cell classification. For instance, one paper used PCA for transfer learning for CNNs with kernel fusion [51] to complete the task of classification in MHSI. This publication made use of the Gabor kernel (which is implemented to obtain spatial features) and the CNN kernel to improvise conventional CNN execution for MHSI classification, with the proposed model showing improved performance. CNN has also been implemented to classify blood cell MHSI in a similar fashion [45], [52], [53], where increased pixel size for the MHSI produced better results with respect to classification accuracy, thus further proving the potential for CNN in MHSI. While all three papers implement pixel-patch input approaches with varying numbers of samples, the proposed two-channel end-to-end

framework [53] provides better results when compared to the combination of modulated Gabor and CNN [52] and the novel CNN implementation [45]. Another publication studies the classification of blood stains from similar appearing objects such as synthetic blood, and tomato concentrate from a forensic sciences point of view [54]. This study tested several standard DL classifiers such as MLP, RNN and CNN (1D, 2D & 3D) with HSI image dataset feeding whole image inputs to the models, with results indicating that 3D CNN outperformed the other algorithms. The CNN model showed promising prospects using spectral patches as an input while also classifying head and neck cancer [35], including even an animal model in a similar setting [55]. One particular paper also proposed a RNN-CNN combined approach for the same domain that performed better than the other CNNs benchmarked in their study [56]. A proposed CNN model also produced successful results by utilizing patches of feature maps for classification of oral cancer diagnosis [57], the performance of which was verified by implementing the same dataset for SVM and DBN. Hybrid CNN models were also observed for classification in MHSI. One particular study used a combination of 2D-3D CNN framework with a patch-based approach for the input to aid brain tumor resection which delivered an overall mean accuracy of 80% [58]. Another publication made use of a similar hybrid model in which pixel patches are fed from the HSI data cube into the model for classification, producing a mean accuracy of 82%. The majority of the proposed CNN models discussed in this section all build upon the traditional architecture for CNN, which better suits the requirements for the medical diagnosis under examination.

## B. DETECTION

Detection techniques in general refer to object detection for a given input image. For MHSI, detection techniques are habitually used for the purpose of detection of malignant cancerous samples, although they are also used for reconstruction of tissue samples. This process is displayed in Fig. 10. While ANN has been used to detect such cancerous samples [59], the majority of detection techniques implemented for MHSI use CNNs for classification of the pixels of the image, which is then used to detect the malign cancer cells/tissues [60], [61]. Both of the aforementioned papers use a simple CNN with spectral signatures as an input to detect head and neck cancer, with one building models from scratch [60] and the other utilizing a pre-trained CNN model [61]. From this, after the pixel-wide classification is obtained from CNNs, it can also be considered as object classification, which is then used for post-processing to detect the presence of cancer or other purposes for the given input sample. One similar study implemented a CNN-based model to reconstruct tissue surface using an endoscopic probe, which displayed potential for practical applications [62]. One study also applied FCN to investigate tissue surface samples using an endoscopic probe in a similar fashion [63]. Another similar study applied dense
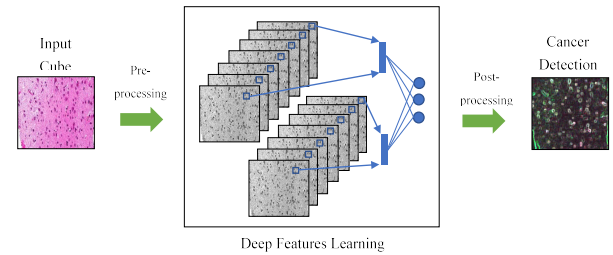


**FIGURE 10.** Standard workflow for cancer detection using deep learning on medical image analysis.

local features (DELF) architecture which also utilizes FCN in its structure for its feature detection and extraction [64].

In recent years, CNN has been particularly useful for MHSI in head and neck squamous cell carcinoma detection [65], [66], although AEN has also been applied for a similar scenario [67]. For the CNN implementations in head and neck cancer detection, one paper implemented an inception-v4 based CNN architecture [65], whereas the other publication utilized an inception-v1 CNN architecture in tandem with a modified HELICoiD and CNN classifier [66], with the former paper producing better results. Another such paper studied the application of CNN in similar domains [68], [69], with the former using 2D-CNN and the latter applying Dense-Blocks in its CNN model, which are part of densely connected neural networks (DenseNet). Application of 2D-CNN was also observed for detection of breast cancer cells detection which also displayed promising results [70]. Implementation of CNN was also observed for aiding brain tumor resection surgeries in real-time amongst the considered papers [71] and similarly towards determining skin cancer detection [72]. Such publications heavily suggest that although CNN is finely suited for classification techniques, as discussed in a prior subsection, it also possesses a potential for detection techniques that support a promising outlook for future research of detection techniques in MHSI.

## C. SEGMENTATION

Segmentation provides outlines for certain parts of images that dictate the position, volume, and size of the relative objects in an image, as discussed in Section 2 of this study. For medical image diagnosis, this is particularly useful, as it could clearly outline certain organs as well as other noteworthy parts of a medical image. This is significant for medical diagnosis in which brain, liver, or other important organs need to be distinguished from a medical image. While segmentation has been extensively used for medical diagnosis over the years [73], [74], in the case of MHSI, we could only find a handful of notable papers that used a segmentation technique.

One of these papers implemented a dense-FCN (FCN being the foundation for U-net [39]) in segmentation for the purpose of retinal image analysis [75]. Fig. 11 depicts a simple graphical representation of FCN for image segmentation. With the usage of *k*-means clustering on the input data, the study was able to lessen the complexity in order to aid
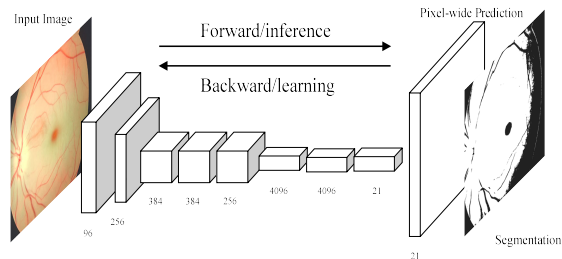
**FIGURE 11.** Classical representation of an FCN for the purposes of segmentation.

the segmentation process and ultimately complete validation against alternate approaches involving other ML algorithms such as SVM and random forest. Its findings suggest that spectral data may provide the opportunity for improvised segmentation results for optic disc and macula segmentation, which is important for retinal imaging analysis, thereby prompting the urge for further research for segmentation techniques for MHSI. Another such study implemented a deformable U-net (dU-Net) to aid sickle cell disease diagnosis by segmenting red blood cells [76]. The proposed model replaces the convolution layers in U-net with deformable convolution to better tackle the shape transformation in objects from the raw images fed into the model. The results obtained from the experimental design in the paper displayed better performance than U-net and other segmentation models, which showcases the prowess of research in segmentation techniques. One additional study made use of a dual-stream U-net variant for tongue tumor detection, with each part of the architecture accepting a certain spectral range of the input, which takes in image patches [77]. The results obtained from experimental procedures observed the fact that although the proposed model was not the best performer, it was significantly close to the best accuracy produced by another variant.

### D. OTHER
DL applications of MHSI go beyond the normal implementation of traditional domains of machine learning. This can be observed in a handful of papers considered in this study. For example, one study utilized GAN with the aid of an autoencoder using MATLAB ML tools in order to determine the tissue oxygen saturation using hyperspectral input data, the results of which are useful for the detection of ischaemia, a fatal disease that affects the blood supply to different organs of the body, particularly the heart muscles [78].

Another similar case in which blood oxygenation is determined using MATLAB tools was discussed in a 2017 study [79]. In this circumstance, the NN fitting tool was used to retrieve the parameters necessary to determine the oxygen saturation levels. In another 2017 study, GAN was employed again to assist in the task of staining lung histology imaging, which was then used to further study the necessary tissue samples [80]. One particular study also made use of GAN to synthesize MHSI from clinical RGB images [81]. The generator in this architecture of conditional GAN (cGAN) is a

modified U-net CNN and the produced HSI is validated using established metrics for single-band real HSI. Lastly, one similar study implements deep convolutional GAN (DCGAN) to generate MHSI relative to skin cancer [82]. This model uses two 3D-convolution layers and one convolution layer which accepts all dimensions in its generator, and the results as discussed in the study look similar to the measured data with the exception of one particular spectral band.

Overall, these studies suggest a broader field of applications of DL for MHSI in the near future. Tables 1 and 2 below consist of the relevant publications we obtained for this paper. Table 1 details the titles of the papers and the category of DL to which the paper pertains, while Table 2 lists the application area of each paper.

## IV. CHALLENGES IN AND FUTURE OF DL MHSI
The boom in deep learning research following the ILSVRC in 2012 has had substantial effects on a variety of disciplines [33], particularly in medical image analysis and diagnosis, as evident from the surge in papers published [88], [89]. While some domains in the medical community have already felt the impact of the applications of deep learning techniques, particularly the domain of radiology, which poses the risk of decline for the profession of practicing radiologists [90], MHSI has yet to experience a similar fate. This may simply be due to the lack of broader researchers of MHSI in general. However, examining the trend observed in the number of publications for deep learning implemented in MHSI, there may be a similar outcome over the coming years. With the unprecedented advancement in general medical image analysis seeming to reach an impasse, as deep learning methodologies augment and improvise efficiency with more accurate results [33], the MHSI profession is also likely to be impacted. Besides, further research for MHSI would focus on unsupervised deep learning algorithm development which has been also a challenging problem.

With such deep-rooted research in deep learning techniques, it is clearly evident that no one technique trumps all others, as the needs and requirements vary from one situation to another. However, CNNs appear to be the prevalent choice, as the bulk of publications considered in this paper utilize it in some way or another. Meanwhile, there are still variants of architectures of CNNs implemented for a particular circumstance, such as in [35] and [66]. Although both investigate the same subject of neck and head cancer, they each use different approaches to tackle the challenge using CNNs. Issues for deep learning for MHSI also stem from several existing DL woes, one of which relates to the broader problems for classification and detection, particularly imbalance of classification for the purpose of object detection. The detection systems first perform a pixel-wide classification, as discussed in the earlier section, which typically causes the class imbalance to be biased towards non-object classes during the training process, which is easier to discern amongst the samples and may cause distortion in the overall detection process.

**TABLE 1.** Papers using deep learning techniques for MHSI.

| Publication Title | Category |
|---|---|
| Cell classification using convolutional neural networks in medical hyperspectral imagery [45] | Classification |
| Hyperspectral imaging for cancer detection and classification [47] | |
| Medical hyperspectral imaging: a review [7] | |
| Deep convolutional neural networks for classifying head and neck cancer using hyperspectral imaging [35] | |
| Deep learning based classification for head and neck cancer detection with hyperspectral imaging in an animal model [55] | |
| Convolutional neural network for medical hyperspectral image classification with kernel fusion [51] | |
| Blood cell classification based on hyperspectral imaging with modulated Gabor and CNN [52] | |
| Medical hyperspectral image classification based on end-to-end fusion deep neural network [53] | |
| Tissue classification of oncologic esophageal resectates based on hyperspectral data [49] | |
| Computer-assisted medical image classification for early diagnosis of oral cancer employing deep learning algorithm [57] | |
| Design of a multilayer neural network for the classification of skin ulcers' hyperspectral images: a proof of concept [48] | |
| Hyperspectral imaging based method for fast characterization of kidney stone types [46] | Classification |
| Design of a multilayer neural network for the classification of skin ulcers' hyperspectral images: a proof of concept [83] | |
| Non-invasive skin cancer diagnosis using hyperspectral imaging for in-situ clinical support [50] | |
| Hyperspectral imaging for colon cancer classification in surgical specimens: towards optical biopsy during image-guided surgery [84] | |
| Deep learning applied to hyperspectral endoscopy for online spectral classification [85] | |

**TABLE 1.** *(Continued.)* Papers using deep learning techniques for MHSI.

| Publication Title | Category |
|---|---|
| Spectral-spatial recurrent-convolutional networks for in-vivo hyperspectral tumor type classification [56] | Detection |
| Blood stain classification with hyperspectral imaging and deep neural networks [54] | |
| Hyperspectral imaging for glioblastoma surgery: improving tumor identification using a deep spectral-spatial approach [58] | |
| Dual-modality endoscopic probe for tissue surface shape reconstruction and hyperspectral imaging enabled by deep neural networks [62] | Detection |
| Probe-based rapid hybrid hyperspectral and tissue surface imaging aided by fully convolutional networks [63] | |
| A dual stream network for tumor detection in hyperspectral images [59] | |
| Adaptive deep learning for head and neck cancer detection using hyperspectral imaging [67] | |
| Hyperspectral imaging of head and neck squamous cell carcinoma for cancer margin detection in surgical specimens from 102 patients using deep learning [65] | |
| Hyperspectral imaging for head and neck cancer detection: specular glare and variance of the tumor margin in surgical specimens [66] | |
| Cancer detection using hyperspectral imaging and evaluation of the superficial tumor margin variance with depth [61] | |
| Surgical aid visualization system for glioblastoma tumor identification based on deep learning and in-vivo hyperspectral images of human patients [71] | |
| Optical biopsy of head and neck cancer using hyperspectral imaging and convolutional neural networks [60] | |
| Convolutional neural networks in skin cancer detection using spatial and spectral domain [72] | Detection |
| Hyperspectral microscopic imaging for automatic detection of head and neck squamous cell carcinoma using histologic image and machine learning [68] | |
| Hyperspectral imaging and deep learning for the detection of breast cancer cells in digitized histological images [70] | |
| Hyperspectral imaging for the detection of glioblastoma tumor cells in H&E slides using convolutional neural networks [86] | |
| Spatio-spectral deep learning methods for in-vivo hyperspectral laryngeal cancer detection [69] | |

**TABLE 1.** *(Continued.)* Papers using deep learning techniques for MHSI.

| | |
|---|---|
| Hyperspectral imaging for skin feature detection: advances in markerless tracking for spine surgery [64] | |
| Detection of tumoral epithelial lesions using hyperspectral imaging and deep learning [87] | |
| Hyperspectral image segmentation of retinal vasculature, optic disc and macula [75] | |
| Automated semantic segmentation of red blood cells for sickle cell disease [76] | Segmentation |
| Tongue tumor detection in hyperspectral images using deep learning semantic segmentation [77] | |
| Towards virtual H&E staining of hyperspectral lung histology images using conditional generative adversarial networks [80] | Other |
| Hyperspectral system for imaging of skin chromophores and blood oxygenation [79] | |
| Estimation of tissue oxygen saturation from RGB images and sparse hyperspectral signals based on conditional generative adversarial network [78] | Other |
| Conditional generative adversarial network for synthesizing hyperspectral images of breast cancer cells from digitized histology [81] | |
| Generating hyperspectral skin cancer imagery using generative adversarial neural network [82] | |

**TABLE 2.** Deep learning methodologies used in MHSI and their applications.

| Methodology | Application |
|---|---|
| CNN | Applied CNN with comparison to SVM for blood cell discrimination [45] |
| | CNN-based model used for endoscopic image reconstruction to enhance surgical guidance [62] |
| | Classifying cancerous tissue samples from neck and head regions using CNN [35] |
| | Detection of neck and head cancerous cells via classification using CNN [55] |
| | Improvisation of CNN using kernel fusion implemented for cell classification [51] |
| | Implementation of CNN for blood cell classification [52] |
| | Two-channel CNN for solving limited-samples problem for CNN models [53] |
| | Use of CNN to detect squamous cell carcinoma between samples from different patients [65] |
| | CNN used for detection of oral cancer [57] |
| | Using specular glare in MHSI along with CNN to detect squamous cell carcinoma [66] |
| | Another study for CNN to detect squamous cell carcinoma [61] |
| | Detection of brain tumor with the aid of CNN [71] |

Given the large amount of untapped potential in deep learning research for MHSI, the key challenge at this time is the uncertainty regarding which DL algorithms should be and can be thoroughly explored and whether the predicted results can be explainable. For instance, we found that classification in MHSI applications has been primarily limited primarily to CNNs [35], [45], [57], thus leaving other methods such as DBNs to be uncharted territory. Detection, on the other hand, mostly consisted of CNNs [60], [62], [65] as well as some instances of FCN [63], while rare cases of utilizing FCN for MHSI segmentation [75]. In the latter two cases, the most logical step forward would be full implementation of the U-net architecture, given its roots in FCN and its success with other medical imaging applications in segmenting features and improving the accuracy of medical diagnoses [91]. This would help to serve as a proficient step forward in advancing the arsenal of deep learning available for MHSI.

Further exploration of other deep learning algorithms in this area, however, is currently limited to another significant challenge, the availability of large, relevant datasets. As detailed later in Appendix B, several of the datasets used in the literature obtained from on-site medical samples

and procedures [35], [61] as well as direct experimentation via imaging systems [53], [62]. While this method of data collection can be useful for researchers who are working directly with medical personnel, this provides a substantial bottleneck for anyone in academic, industrial, or government backgrounds that are not closely linked to the medical field, thereby limiting the scope of researchers, data scientists, and engineers who can provide the potential expertise and innovation needed to bring a greater breadth and deeper expertise of deep learning methods to the table. Overall, only one easily accessible repository was utilized by researchers that we found [57]. Thus, in order to expand the deep learning tools available for medical hyperspectral imaging, the medical

**TABLE 2.** *(Continued.)* **Deep learning methodologies used in MHSI and their applications.**

| CNN | Detecting carcinoma thyroid sample with the aid of CNN [60] |
|---|---|
| | Different CNN models compared to one another for classifying skin cancer from patient data HIS [72] |
| | CNN utilized to classify and detect squamous cell carcinoma [68] |
| | CNN used to classify and detect breast cancer cells [70] |
| | CNN implemented for detection of Glioblastoma cells from Hematoxylin & Eosin tissue sample [86] |
| | In-vivo Laryngeal cancer detection based on CNN [69] |
| | Convolutional based RetinaNet model implemented to classify and detect tumors in epithelial tissue [87] |
| | Implemented a hybrid CNN model to classify colon tumor in order to aid surgical guidance [84] |
| | Five-layer CNN applied to classify endoscopy HSI [85] |
| | Study of classification for blood and similar appearing substances from HSI with CNN,RNN, MLP [54] |
| | Proposed framework of 3D-2D CNN-based approach to classify brain tumors [58] |
| ANN | Implementation of ANN and SVM for cancerous cell HSI [47] |
| | This review paper discusses the use of ANN for classification for MHSI [7] |
| | Classifying cutaneous ulcer HIS using feedforward ANN [48] |
| | ANN used to classify kidney stone tissue samples [46] |
| | ANN utilized to classify cutaneous ulcers' hyperspectral images in 4 kind of causes: occlusive vasculopathy [48] |
| | ANN used as part of proposed framework for classification of skin samples [50] |
| AEN | Use of AEN to detect cancer in a tissue sample [67] |

**TABLE 2.** *(Continued.)* **Deep learning methodologies used in MHSI and their applications.**

| FCN | Segmentation for the automatic retinal image analysis [75] |
|---|---|
| | Spot detection for surgical endoscopic tissue sample aided by FCN [63] |
| | Deep local features (DELF) and FCN implemented to detect skin features [64] |
| GAN | Virtual staining for lung histology images using GANs [80] |
| | GAN-inspired model used to estimate the tissue oxygen saturation [78] |
| | Implementation of GAN to synthesize MHSI from RGB images of Breast cell samples [81] |
| | GAN implemented as a generator for skin cancer HSI [82] |
| NN | Matlab NN toolkit used to characterize of skin using 2d mapping of skin chromophore distribution [79] |
| | NN with 2 hidden layers used as a classifier to combine structural and spectral data for tumor detection in tongue [59] |
| MLP | Evaluation of different supervised algorithms, including MLP, to analyze tissue samples of esophago-gastric resectates [49] |
| RCN | Application of multiple CNN and RCN to cancerous tissue HSI for comparative analysis [85] |
| U-net | Classification of red blood cells for Sickle Cell Disease with the use of deformable U-net (dU-Net) [76] |
| | Implementation of U-net variant for segmentation of tongue squamous cell carcinoma [77] |

field will need to further engage in the mindset of making MHSI data available through repositories that balance ease of access with sufficient compliance with all needed regulatory requirements.

## V. CONCLUSION

Despite the boom in deep learning, its rigorous applications in medical image analysis, and the benefit of hyperspectral imaging for medical analysis, there have not yet been any papers published that review the publications dedicated towards the implementation of deep learning for medical hyperspectral image analysis. In this paper, we discussed the deep learning techniques for medical hyperspectral imaging and relevant papers published relative to the topic within the year range of 2012-2020. In short, similar to the trend observed for deep learning since the iconic ILSVRC 2012, there was a definite boost in research and papers published for
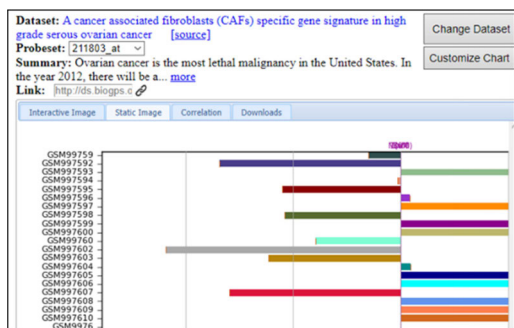
**FIGURE 12.** Sample dataset from BioGPS repository: collection of genome signatures of ovarian tissue that can be utilized to identify ovarian cancer associated fibroblasts (CAFs) gene signatures [92].

deep learning for MHSI and medical image analysis in general. We also discussed the different methodologies discussed in all the papers we found as well as what the future in DL for MHSI may look like. The trend for the majority of papers implementing DL for MHSI seems to be paved by the use of CNNs to classify blood cells/tissue samples in order to aid cancer detection and analysis. We could only find one paper that discussed the use of FCN for segmentation rationales of retinal imaging. Lastly, there were also isolated uses of GAN and MATLAB tools to determine tissue oxygenation levels that could potentially be used for detecting ischaemia (disease directly dependent on blood supply to vital organs) or even in staining of lung histology imaging.

## APPENDIX A
## SEARCH CRITERIA

Google Scholar was implemented to find the relative publications considered for this paper. The key search words included during our search are ''deep learning'' and ''medical hyperspectral imaging''; we found that word searches for topics such as specific techniques yielded more inaccurate results relative to our purpose. We selected the most relevant papers from a certain range of search results. In addition to Google Scholar, we also searched for the same search words on the publisher's own search engines for the papers considered for this article, which resulted in the discovery of papers that previously did not appear in Google Scholar.

## APPENDIX B
## DATASETS

The majority of datasets utilized by the publications were obtained either directly through experimentation using various imaging systems or via contribution from hospitals, laboratories, or clinical storage. Some examples of testing systems implemented include CRI Maestro for vivo imaging system [67], and more commonly used Liquid Crystal Tunable Filters (LCTF) [51]–[53], [78], and Hybrid Endoscopic Apparatus (ICL SLHSI) [62]. Several papers also used actual medical samples, such as patients undergoing surgical cancer resection [35], [61] and other contributions of local patient samples from hospitals, medical centers, and laboratories.

The only largely available repository in use by a paper was BioGPS UCI repository [57]. Fig. 12 shows a small sample representation of a dataset from this repository.

## APPENDIX C
## SOFTWARE

Many software packages were implemented across all the publications discussed in this paper, the majority of which implemented Tensorflow (wherever stated). Tensorflow is an open-source machine learning platform based on Python, which is supported by its vast number of libraries, tools, and community resources. The complete list of software packages and libraries along with the papers utilizing them can be found below-

| Software | Utilizing Publications |
|---|---|
| Statistica | [46] |
| Unscrambler (for PCA/ ANN) | [46] |
| Matlab (data processing / implementing NNs) | [52] [45] [51] [46] [47] [79] [50] |
| Tensorflow (Python) | [52] [61] [51] [35] [62] [66] [65] [53] [60] [71] [81] [87] [70] |
| Keras (Python) | [72] [53] [70] |
| Scikit (Python) | [49] [54] |
| PyTorch (Python) | [54] |
| Caffe | [45] |
| Ilastik software | [76] |

## REFERENCES

[1] I. G. Stiell, G. A. Wells, K. Vandemheen, C. Clement, H. Lesiuk, A. Laupacis, R. D. McKnight, R. Verbeek, R. Brison, D. Cass, M. A. Eisenhauer, G. H. Greenberg, and J. Worthington, ''The Canadian CT head rule for patients with minor head injury,'' *Lancet*, vol. 357, no. 9266, pp. 1391–1396, May 2001.

[2] R. Lawaczeck, V. Arkadiev, F. Diekmann, and M. Krumrey, ''Monochromatic X-rays in digital mammography,'' *Investigative Radiol.*, vol. 40, no. 1, pp. 33–39, 2005.

[3] K. Doi, ''Computer-aided diagnosis in medical imaging: Historical review, current status and future potential,'' *Computerized Med. Imag. Graph.*, vol. 31, nos. 4–5, pp. 198–211, Jun. 2007.

[4] F. E.-Z.-A. El-Gamal, M. Elmogy, and A. Atwan, ''Current trends in medical image registration and fusion,'' *Egyptian Informat. J.*, vol. 17, no. 1, pp. 99–124, Mar. 2016.

[5] A. Stylianou and M. A. Talias, ''Nanotechnology-supported THz medical imaging,'' *FResearch*, vol. 2, p. 100, Mar. 2013.

[6] M. A. Calin, S. V. Parasca, D. Savastru, and D. Manea, ''Hyperspectral imaging in the medical field: Present and future,'' *Appl. Spectrosc. Rev.*, vol. 49, no. 6, pp. 435–447, Aug. 2014.

[7] G. Lu and B. Fei, ''Medical hyperspectral imaging: A review,'' *J. Biomed. Opt.*, vol. 19, no. 1, Jan. 2014, Art. no. 010901.

[8] P. Sidike, V. K. Asari, and V. Sagan, ''Progressively expanded neural network (PEN Net) for hyperspectral image classification: A new neural network paradigm for remote sensing image analysis,'' *ISPRS J. Photogramm. Remote Sens.*, vol. 146, pp. 161–181, Dec. 2018.

[9] J. Ren, J. Zabalza, S. Marshall, and J. Zheng, ''Effective feature extraction and data reduction in remote sensing using hyperspectral imaging [applications corner],'' *IEEE Signal Process. Mag.*, vol. 31, no. 4, pp. 149–154, Jul. 2014.

[10] D. Lorente, N. Aleixos, J. Gómez-Sanchis, S. Cubero, O. L. García-Navarrete, and J. Blasco, ''Recent advances and applications of hyperspectral imaging for fruit and vegetable quality assessment,'' *Food Bioprocess Technol.*, vol. 5, no. 4, pp. 1121–1142, May 2012.

[11] Y.-Z. Feng and D.-W. Sun, "Application of hyperspetral imaging in food safety inspection and control: A review," *Crit. Rev. Food Sci. Nutrition*, vol. 52, no. 11, pp. 1039–1058, 2012.

[12] D. Wu and D.-W. Sun, "Advanced applications of hyperspectral imaging technology for food quality and safety analysis and assessment: A review—Part I: Fundamentals," *Innov. Food Sci. Emerg. Technol.*, vol. 19, pp. 1–14, Jul. 2013.

[13] S. Paheding, Y. Diskin, S. Arigela, and V. K. Asari, "Visibility improvement of shadow regions using hyperspectral band integration," *Proc. SPIE*, vol. 9244, Oct. 2014, Art. no. 92440V.

[14] M. S. Alam, R. P. Gollapalli, and S. Paheding, "Identification and detection of oil and oil-derived substances at the surface and subsurface levels via hyperspectral imaging," *Proc. SPIE*, vol. 8398, Apr. 2012, Art. no. 839802.

[15] M. S. Alam and S. Paheding, "Trends in oil spill detection via hyperspectral imaging," in *Proc. 7th Int. Conf. Elect. Comput. Eng.*, Dhaka, Bangladesh, 2012, pp. 858–862.

[16] A. Essa, P. Sidike, and V. Asari, "Volumetric directional pattern for spatial feature extraction in hyperspectral imagery," *IEEE Geosci. Remote Sens. Lett.*, vol. 14, no. 7, pp. 1056–1060, Jul. 2017.

[17] S. Paheding, C. Chen, V. Asari, Y. Xu, and W. Li, "Classification of hyperspectral image using multiscale spatial texture features," in *Proc. IEEE 8th Workshop Hyperspectral Image Signal Process. Evol. Remote Sens.*, Aug. 2016, pp. 1–4.

[18] S. Paheding, V. K. Asari, and M. S. Alam, "Multiclass object detection with single query in hyperspectral imagery using class-associative spectral fringe-adjusted joint transform correlation," *IEEE Trans. Geosci. Remote Sens.*, vol. 54, no. 2, pp. 1196–1208, Sep. 2016.

[19] D. Manolakis and G. Shaw, "Detection algorithms for hyperspectral imaging applications," *IEEE Signal Process. Mag.*, vol. 19, no. 1, pp. 29–43, Aug. 2002.

[20] S. Paheding, V. K. Asari, and M. S. Alam, "Multiple object detection in hyperspectral imagery using spectral fringe-adjusted joint transform correlator," *Proc. SPIE*, vol. 9405, Feb. 2015, Art. no. 940502.

[21] C. Fischer and I. Kakoulli, "Multispectral and hyperspectral imaging technologies in conservation: Current research and potential applications," *Stud. Conservation*, vol. 51, no. 1, pp. 3–16, Jun. 2006.

[22] S. V. Panasyuk, S. Yang, D. V. Faller, D. Ngo, R. A. Lew, J. E. Freeman, and A. E. Rogers, "Medical hyperspectral imaging to facilitate residual tumor identification during surgery," *Cancer Biol. Therapy*, vol. 6, no. 3, pp. 439–446, Mar. 2007.

[23] G. Lu, J. V. Little, X. Wang, H. Zhang, M. R. Patel, C. C. Griffith, M. W. El-Deiry, A. Y. Chen, and B. Fei, "Detection of head and neck cancer in surgical specimens using quantitative hyperspectral imaging," *Clin. Cancer Res.*, vol. 23, no. 18, pp. 5426–5436, Sep. 2017.

[24] S. Kiyotoki, J. Nishikawa, T. Okamoto, K. Hamabe, M. Saito, A. Goto, Y. Fujita, Y. Hamamoto, Y. Takeuchi, S. Satori, and I. Sakaida, "New method for detection of gastric cancer by hyperspectral imaging: A pilot study," *J. Biomed. Opt.*, vol. 18, no. 2, Feb. 2013, Art. no. 026010.

[25] R. Pike, S. K. Patton, G. Lu, L. V. Halig, D. Wang, Z. G. Chen, and B. Fei, "A minimum spanning forest based hyperspectral image classification method for cancerous tissue detection," *Proc. SPIE*, vol. 9034, pp. 15–20, Mar. 2014.

[26] Y. LeCun, Y. Bengio, and G. Hinton, "Deep learning," *Nature*, vol. 521, pp. 436–444, May 2015.

[27] G. Lu, X. Qin, D. Wang, S. Muller, H. Zhang, A. Chen, Z. G. Chen, and B. Fei, "Hyperspectral imaging of neoplastic progression in a mouse model of oral carcinogenesis," *Proc. SPIE*, vol. 9788, Mar. 2016, Art. no. 978812.

[28] A. Madooei, R. M. Abdlaty, L. Doerwald-Munoz, J. Hayward, M. S. Drew, Q. Fang, and J. Zerubia, "Hyperspectral image processing for detection and grading of skin erythema," *Proc. SPIE*, vol. 10133, pp. 1–7, Feb. 2017.

[29] H. Akbari, Y. Kosugi, K. Kojima, and N. Tanaka, "Blood vessel detection and artery-vein differentiation using hyperspectral imaging," in *Proc. Annu. Int. Conf. IEEE Eng. Med. Biol. Soc.*, Sep. 2009, pp. 1461–1464.

[30] L. Zhi, D. Zhang, J.-Q. Yan, Q.-L. Li, and Q.-L. Tang, "Classification of hyperspectral medical tongue images for tongue diagnosis," *Comput. Med. Imag. Graph.*, vol. 31, no. 8, pp. 672–678, Dec. 2007.

[31] S. Vyas, A. Banerjee, L. Garza, S. Kang, and P. Burlina, "Hyperspectral signature analysis of skin parameters," *Proc. SPIE*, vol. 8670, Feb. 2013, Art. no. 867002.

[32] M. Z. Alom, T. M. Taha, C. Yakopcic, S. Westberg, S. Paheding, M. S. Nasrin, B. C. V. Essen, A. A. S. Awwal, and V. K. Asari, "The history began from AlexNet: A comprehensive survey on deep learning approaches," 2018.

[33] M. Z. Alom, T. M. Taha, C. Yakopcic, S. Westberg, P. Sidike, M. S. Nasrin, M. Hasan, B. C. Van Essen, A. A. S. Awwal, and V. K. Asari, "A state-of-the-art survey on deep learning theory and architectures," *Electronics*, vol. 8, no. 3, p. 292, Mar. 2019.

[34] M. G. Crowson, J. Ranisau, A. Eskander, A. Babier, B. Xu, R. R. Kahmke, J. M. Chen, and T. C. Y. Chan, "A contemporary review of machine learning in otolaryngology–head and neck surgery," *Laryngoscope*, vol. 130, no. 1, pp. 45–51, 2019.

[35] M. Halicek, G. Lu, J. V. Little, X. Wang, M. Patel, C. C. Griffith, M. W. El-Deiry, A. Y. Chen, and B. Fei, "Deep convolutional neural networks for classifying head and neck cancer using hyperspectral imaging," *J. Biomed. Opt.*, vol. 22, no. 6, 2017, Art. no. 060503.

[36] A. Krizhevsky, I. Sutskever, and G. E. Hinton, "ImageNet classification with deep convolutional neural networks," in *Proc. Adv. Neural Inf. Process. Syst.*, 2012, pp. 1097–1105.

[37] H. Wang and B. Raj, *On the Origin of Deep Learning*. Pittsburgh, PA, USA: Carnegie Mellon Univ., 2017.

[38] Y. Lecun, L. Bottou, Y. Bengio, and P. Haffner, "Gradient-based learning applied to document recognition," *Proc. IEEE*, vol. 86, no. 11, pp. 2278–2324, Nov. 1998.

[39] O. Ronneberger, P. Fischer, and T. Brox, "U-Net: Convolutional networks for biomedical image segmentation," in *Medical Image Computing and Computer-Assisted Intervention—MICCAI*. Cham, Switzerland: Springer, 2015, pp. 234–241.

[40] W. Yin, K. Kann, M. Yu, and H. Schutze, "Comparative study of CNN and RNN for natural language processing," Feb. 2017.

[41] M. Z. Alom, V. Bontupalli, and T. M. Taha, "Intrusion detection using deep belief networks," in *Proc. Nat. Aerosp. Electron. Conf. (NAECON)*, Dayton, OH, USA, 2015, pp. 339–344.

[42] R. Sarikaya, G. E. Hinton, and A. Deoras, "Application of deep belief networks for natural language understanding," *IEEE/ACM Trans. Audio, Speech, Language Process.*, vol. 22, no. 4, pp. 778–784, Apr. 2014.

[43] A. Khatami, A. Khosravi, T. Nguyen, C. P. Lim, and S. Nahavandi, "Medical image analysis using wavelet transform and deep belief networks," *Expert Syst. Appl.*, vol. 86, pp. 190–198, sNov. 2017.

[44] S. A. Jalalifar, H. Hasani, and H. Aghajan, *Speech-Driven Facial Reenactment Using Conditional Generative Adversarial Networks*. Mar. 2018.

[45] X. Li, W. Li, X. Xu, and W. Hu, "Cell classification using convolutional neural networks in medical hyperspectral imagery," in *Proc. 2nd Int. Conf. Image, Vis. Comput. (ICIVC)*, Chengdu, China, 2017, pp. 501–504.

[46] F. Blanco, M. López-Mesas, S. Serranti, G. Bonifazi, J. Havel, and M. Valiente, "Hyperspectral imaging based method for fast characterization of kidney stone types," *J. Biomed. Opt.*, vol. 17, no. 7, 2012, Art. no. 076027.

[47] M. Nathan, A. Kabatznik, and A. Mahmood, "Hyperspectral imaging for cancer detection and classification," in *Proc. 3rd Biennial South Afr. Biomed. Eng. Conf. (SAIBMEC)*, Stellenbosch, South Africa, 2018, pp. 1–4.

[48] D. C. Jaramillo, J. E. Escobar, J. Galeano, and M. C. Torres-Madronero, "Design of a multilayer neural network for the classification of skin ulcers' hyperspectral images: A proof of concept," in *Proc. 15th Int. Symp. Med. Inf. Process. Anal.*, Medellín, Colombia, 2019.

[49] M. Maktabi, H. Köhler, M. Ivanova, B. Jansen-Winkeln, J. Takoh, S. Niebisch, S. M. Rabe, T. Neumuth, I. Gockel, and C. Chalopin, "Tissue classification of oncologic esophageal resectates based on hyperspectral data," *Int. J. Comput. Assist. Radiol. Surg.*, vol. 14, no. 10, pp. 1651–1661, 2019.

[50] R. Leon, B. Martinez-Vega, H. Fabelo, S. Ortega, V. Melian, I. Castaño, G. Carretero, P. Almeida, A. Garcia, E. Quevedo, J. A. Hernandez, B. Clavo, and G. M. Callico, "Non-invasive skin cancer diagnosis using hyperspectral imaging for *in-situ* clinical support," *J. Clin. Med.*, vol. 9, no. 6, p. 1662, Jun. 2020.

[51] Q. Huang, W. Li, and X. Xie, "Convolutional neural network for medical hyperspectral image classification with kernel fusion," in *Proc. Int. Conf. Biol. Inf. Biomed. Eng.*, Shanghai, China, Jun. 2018, pp. 1–4.

[52] Q. Huang, W. Li, B. Zhang, Q. Li, R. Tao, and N. H. Lovell, "Blood cell classification based on hyperspectral imaging with modulated Gabor and CNN," *IEEE J. Biomed. Health Informat.*, vol. 24, no. 1, pp. 160–170, Jan. 2020.

[53] X. Wei, W. Li, M. Zhang, and Q. Li, "Medical hyperspectral image classification based on end-to-end fusion deep neural network," *IEEE Trans. Instrum. Meas.*, vol. 68, no. 11, pp. 4481–4492, Nov. 2019.

[54] K. Książek, M. Romaszewski, P. Głomb, B. Grabowski, and M. Cholewa, "Blood stain classification with hyperspectral imaging and deep neural networks," *Sensors*, vol. 20, no. 22, p. 6666, Nov. 2020.

[55] L. Ma, G. Lu, D. Wang, X. Wang, Z. G. Chen, S. Muller, A. Chen, and B. Fei, "Deep learning based classification for head and neck cancer detection with hyperspectral imaging in an animal model," in *Proc. Med. Imag. Biomed. Appl. Mol., Struct., Funct. Imag.*, Mar. 2017, Art. no. 101372G.

[56] M. Bengs, N. Gessert, W. Laffers, D. Eggert, S. Westermann, N. A. Mueller, A. O. H. Gerstner, C. Betz, and A. Schlaefer, "Spectral-spatial recurrent-convolutional networks for *in-vivo* hyperspectral tumor type Classification," in *Proc. Med. Image Comput.-Assist. Intervent. (MICCAI)*, Lima, Peru, 2020, pp. 690–699.

[57] P. R. Jeyaraj and E. R. S. Nadar, "Computer-assisted medical image classification for early diagnosis of oral cancer employing deep learning algorithm," *J. Cancer Res. Clin. Oncol.*, vol. 145, no. 4, pp. 829–837, Apr. 2019.

[58] F. Manni, F. van der Sommen, H. Fabelo, S. Zinger, C. Shan, E. Edström, A. Elmi-Terander, S. Ortega, G. Marrero Callicó, and P. H. N. de With, "Hyperspectral imaging for glioblastoma surgery: Improving tumor identification using a deep spectral-spatial approach," *Sensors*, vol. 20, no. 23, p. 6955, Dec. 2020.

[59] P. Weijtmans, C. Shan, T. Tan, S. B. D. Koning, and T. Ruers, "A dual stream network for tumor detection in hyperspectral images," in *Proc. IEEE 16th Int. Symp. Biomed. Imag.*, Venice, Italy, Apr. 2019, pp. 1256–1259.

[60] M. Halicek, J. V. Little, X. Wang, A. Y. Chen, and B. Fei, "Optical biopsy of head and neck cancer using hyperspectral imaging and convolutional neural networks," *J. Biomed. Opt.*, vol. 24, no. 3, 2019, Art. no. 036007.

[61] M. Halicek, H. Fabelo, S. Ortega, J. V. Little, X. Wang, A. Y. Chen, G. M. Callico, L. L. Myers, B. D. Sumer, and B. Fei, "Cancer detection using hyperspectral imaging and evaluation of the superficial tumor margin variance with depth," *Proc. SPIE*, vol. 10951, Mar. 2019, Art. no. 109511A.

[62] J. Lin, N. T. Clancy, J. Qi, Y. Hu, T. Tatla, D. Stoyanov, L. Maier-Hein, and D. S. Elson, "Dual-modality endoscopic probe for tissue surface shape reconstruction and hyperspectral imaging enabled by deep neural networks," *Med. Image Anal.*, vol. 48, pp. 162–176, Aug. 2018.

[63] J. Lin, N. T. Clancy, X. Sun, J. Qi, M. Janatka, D. Stoyanov, and D. S. Elson, "Probe-based rapid hybrid hyperspectral and tissue surface imaging aided by fully convolutional networks," in *Proc. Med. Image Comput.-Assist. Intervent. (MICCAI)*, 2016, pp. 414–422.

[64] F. Manni, F. van der Sommen, S. Zinger, C. Shan, R. Holthuizen, M. Lai, G. Buström, R. J. M. Hoveling, E. Edström, A. Elmi-Terander, and P. H. N. de With, "Hyperspectral imaging for skin feature detection: Advances in markerless tracking for spine surgery," *Appl. Sci.*, vol. 10, no. 12, p. 4078, Jun. 2020.

[65] M. Halicek, J. D. Dormer, J. V. Little, A. Y. Chen, L. Myers, B. D. Sumer, and B. Fei, "Hyperspectral imaging of head and neck squamous cell carcinoma for cancer margin detection in surgical specimens from 102 patients using deep learning," *Cancers*, vol. 11, no. 9, p. 1367, Sep. 2019.

[66] M. Halicek, H. Fabelo, S. Ortega, J. V. Little, X. Wang, A. Y. Chen, G. M. Callico, L. Myers, B. D. Sumer, and B. Fei, "Hyperspectral imaging for head and neck cancer detection: Specular glare and variance of the tumor margin in surgical specimens," *J. Med. Imag.*, vol. 6, no. 3, 2019, Art. no. 035004.

[67] L. Ma, G. Lu, D. Wang, X. Qin, Z. G. Chen, and B. Fei, "Adaptive deep learning for head and neck cancer detection using hyperspectral imaging," *Vis. Comput. Ind., Biomed., Art*, vol. 2, no. 18, pp. 1–12, Dec. 2019.

[68] L. Ma, M. Halicek, X. Zhou, J. Dormer, and B. Fei, "Hyperspectral microscopic imaging for automatic detection of head and neck squamous cell carcinoma using histologic image and machine learning," *Proc. SPIE*, vol. 11320, Mar. 2020, Art. no. 113200W.

[69] M. Bengs, N. G. S. Westermann, D. Eggert, A. O. H. Gerstner, N. A. Mueller, C. Betz, W. Laffers, and A. Schlaefer, "Spatio-spectral deep learning methods for *in-vivo* hyperspectral laryngeal cancer detection," *Proc. SPIE*, vol. 11314, Mar. 2020, Art. no. 113141L.

[70] S. Ortega, M. Halicek, H. Fabelo, R. Guerra, C. Lopez, M. Lejeune, F. Godtliebsen, G. M. Callico, and B. Fei, "Hyperspectral imaging and deep learning for the detection of breast cancer cells in digitized histological images," *Proc. SPIE*, vol. 11320, Mar. 2020, Art. no. 113200V.

[71] H. Fabelo, M. Halicek, S. Ortega, A. Szolna, J. Morera, R. Sarmiento, G. M. Callico, and B. Fei, "Surgical aid visualization system for glioblastoma tumor identification based on deep learning and *in-vivo* hyperspectral images of human patients," *Proc. SPIE*, vol. 10951, Mar. 2019, Art. no. 1095110.

[72] I. Pölönen, S. Rahkonen, L. Annala, and N. Neittaanmäki, "Convolutional neural networks in skin cancer detection using spatial and spectral domain," *Proc. SPIE*, vol. 10851, Feb. 2019, Art. no. 108510B.

[73] L. Bi, D. Feng, and J. Kim, "Dual-path adversarial learning for fully convolutional network (FCN)-based medical image segmentation," *Vis. Comput.*, vol. 34, nos. 6–8, pp. 1043–1052, Jun. 2018.

[74] Y. Shen, Z. Fang, Y. Gao, N. Xiong, C. Zhong, and X. Tang, "Coronary arteries segmentation based on 3D FCN with attention gate and level set function," *IEEE Access*, vol. 7, pp. 42826–42835, Mar. 2019.

[75] A. Garifullin, P. Koobi, P. Ylitepsa, K. Adjers, M. Hauta-Kasari, H. Uusitalo, and L. Lensu, "Hyperspectral image segmentation of retinal vasculature, optic disc and macula," in *Proc. Digit. Image Comput. Techn. Appl. (DICTA)*, Canberra, ACT, Australia, 2018, pp. 1–5.

[76] M. Zhang, X. Li, M. Xu, and Q. Li, "Automated semantic segmentation of red blood cells for sickle cell disease," *IEEE J. Biomed. Health Informat.*, vol. 24, no. 11, pp. 3095–3102, Nov. 2020.

[77] S. Trajanovski, C. Shan, P. J. C. Weijtmans, S. G. B. de Koning, and T. J. M. Ruers, "Tongue tumor detection in hyperspectral images using deep learning semantic segmentation," *IEEE Trans. Biomed. Eng.*, vol. 68, no. 4, pp. 1330–1340, Apr. 2021.

[78] Q. Li, J. Lin, N. T. Clancy, and D. S. Elson, "Estimation of tissue oxygen saturation from RGB images and sparse hyperspectral signals based on conditional generative adversarial network," *Int. J. Comput. Assist. Radiol. Surg.*, vol. 14, pp. 987–995, Mar. 2019.

[79] E. Zherebtsov, A. Popov, A. Doronin, I. Meglinski, and A. Bykov, "Hyperspectral system for imaging of skin chromophores and blood oxygenation," in *Proc. Eur. Conf. Biomed. Opt.*, Münich, Germany, 2017.

[80] N. Bayramoglu, M. Kaakinen, L. Eklund, and J. Heikkila, "Towards virtual H&E staining of hyperspectral lung histology images using conditional generative adversarial networks," in *Proc. IEEE Int. Conf. Comput. Vis. (ICCV)*, Venice, Italy, Oct. 2017, pp. 64–71.

[81] M. Halicek, S. Ortega, H. Fabelo, C. Lopez, M. Lejeune, G. M. Callico, and B. Fei, "Conditional generative adversarial network for synthesizing hyperspectral images of breast cancer cells from digitized histology," *Proc. SPIE*, vol. 11320, Mar. 2020, Art. no. 113200U.

[82] L. Annala, N. Neittaanmäki, J. Paoli, O. Zaar, and I. Polonen, "Generating hyperspectral skin cancer imagery using generative adversarial neural network," in *Proc. 42nd Annu. Int. Conf. IEEE Eng. Med. Biol. Soc. (EMBC)*, Jul. 2020, pp. 1600–1603.

[83] D. C. Jaramillo, J. E. Escobar, J. Galeano, and M. C. Torres-Madronero, "A review of the medical hyperspectral imaging systems and unmixing algorithms' in biological tissues," in *Proc. 15th Int. Symp. Med. Inf. Process. Anal.*, Medelin, Colombia, vol. 11330, 2020.

[84] F. Manni, R. Fonolla, F. V. der Sommen, S. Zinger, C. Shan, E. Kho, S. B. de Koning, T. Ruers, and P. H. N. de With, "Hyperspectral imaging for colon cancer classification in surgical specimens: Towards optical biopsy during image-guided surgery," in *Proc. 42nd Annu. Int. Conf. IEEE Eng. Med. Biol. Soc. (EMBC)*, Montreal, QC, Canada, Jul. 2020, pp. 1169–1173.

[85] A. Grigoroiu, J. Yoon, and S. E. Bohndiek, "Deep learning applied to hyperspectral endoscopy for online spectral classification," *Sci. Rep.*, vol. 10, p. 3947, Mar. 2020.

[86] S. Ortega, M. Halicek, H. Fabelo, R. Camacho, M. D. L. L. Plaza, F. Godtliebsen, G. M. Callicó, and B. Fei, "Hyperspectral imaging for the detection of glioblastoma tumor cells in H&E slides using convolutional neural networks," *Sensors*, vol. 20, no. 7, p. 1911, Mar. 2020.

[87] D. V. de Lucena, A. da Silva Soares, C. J. Coelho, I. J. Wastowski, and A. R. G. Filho, "Detection of tumoral epithelial lesions using hyperspectral imaging and deep learning," in *Proc. Comput. Sci. (ICCS)*, Amsterdam, The Netherlands, 2020, pp. 599–612.

[88] G. Litjens, T. Kooi, B. E. Bejnordi, A. A. A. Setio, F. Ciompi, M. Ghafoorian, J. A. W. M. van der Laak, B. van Ginneken, and C. I. Sánchez, "A survey on deep learning in medical image analysis," *Med. Image Anal.*, vol. 42, pp. 60–88, Dec. 2017.

[89] N. Siddique, P. Sidike, C. Elkin, and V. Devabhaktuni, "U-net and its variants for medical image segmentation: Theory and applications," 2020, *arXiv:2011.01118*. [Online]. Available: http://arxiv.org/abs/2011.01118

[90] C. Liew, "The future of radiology augmented with artificial intelligence: A strategy for success," *Eur. J. Radiol.*, vol. 102, pp. 152–156, May 2018.

[91] G. Du, X. Cao, J. Liang, X. Chen, and Y. Zhan, "Medical image segmentation based on U-net: A review," *J. Imag. Sci. Technol.*, vol. 64, no. 2, pp. 20508-1–20508-12, 2020.

[92] T.-L. Yeung, K.-K. Wong, M. J. Birrer, and S. C. Mok. (Sep. 19, 2014). *Dataset: A Cancer Associated Fibroblasts (CAFs) Specific Gene Signature in High Grade Serous Ovarian Cancer*. [Online]. Available: http://biogps.org/dataset/E-GEOD-40595/a-cancer-associated-fibroblasts-cafs-specific-gene/

**UZAIR KHAN** received the B.S. degree in electrical engineering from Minnesota State University, Mankato, in 2018, and the M.S. degree in electrical and computer engineering from Purdue University Northwest, in 2020. He was an Active Member of the IEEE student branches while pursuing his degrees. He led the student branch at Minnesota State University as a Vice-Chair, from 2017 to 2018. His research interests include machine learning, digital image processing, the embedded IoT devices, statistical analysis, and data science.

**SIDIKE PAHEDING** received the Ph.D. degree in electrical engineering from the University of Dayton. He was a Visiting Assistant Professor with Purdue University Northwest. He is currently an Assistant Professor with the Department of Applied Computing, Michigan Technological University. His research interests include image/video processing, machine learning, deep learning, computer vision, and remote sensing. He is an Associate Editor of the Springer journal *Signal, Image, and Video Processing*, and ASPRS Journal *Photogrammetric Engineering & Remote Sensing*. He serves as a guest editor/reviewer for several reputed journals.

**COLIN P. ELKIN** (Member, IEEE) received the B.S. degree in electrical engineering from The University of Tulsa, in 2013, and the M.S. and Ph.D. degrees in computer science and engineering from The University of Toledo, in 2015 and 2018, respectively. His Ph.D. dissertation was supported by the Air Force Research Laboratory (AFRL) through two research awards, a Dayton Area Graduate Studies Institute (DAGSI) fellowship and an AFRL subcontract through Soar Technology, Inc. He joined the Electrical and Computer Engineering Department, Purdue University Northwest, as a Visiting Instructor, in 2018, and as a Visiting Assistant Professor, where he has been an Assistant Professor, since 2019. He has published more than ten peer-reviewed conferences, journals, and poster papers. His past and present research has been funded by the Department of Defense (DoD), NSF, the Ohio Federal Research Network (OFRN), and industry. His research interests include artificial intelligence, data science, machine learning, optimization techniques, human factors, modeling and simulation, engineering education, and software engineering. He joined IEEE as a Graduate Student Member, in 2014, and has been a regular Member, since 2018.

**VIJAYA KUMAR DEVABHAKTUNI** (Senior Member, IEEE) received the B.Eng. degree in electronics and electrical engineering and the M.Sc. degree in physics from the Birla Institute of Technology Science, Pilani, India, in 1996, and the Ph.D. degree in electronics from Carleton University, Ottawa, ON, Canada, in 2003. He held the Natural Sciences and Engineering Research Council of Canada (NSERC) Postdoctoral Fellowship and spent the tenure researching with Dr. J. W. Haslett at the University of Calgary, Calgary, AB, Canada, from 2003 to 2004. He taught at Penn State Erie Behrend, Erie, PA, USA, in 2005. From 2005 to 2008, he held the prestigious Canada Research Chair in Computer-Aided High-Frequency Modeling & Design, Concordia University, Montreal, QC, Canada. He joined the Department of Electrical Engineering and Computer Science, University of Toledo, Toledo, OH, USA, as an Associate Professor, in 2008, and was promoted to a Professor, in 2013. He joined the Department of Electrical and Computer Engineering, Purdue University Northwest, Hammond, IN, USA, as a Chair, in 2018. He secured external funding close to U.S. five million in his research areas (sponsoring agencies include AFOSR, AFRL, CFI, NASA, NIST, NSERC, NSF, ONR, and industry). He has coauthored 250 peer-reviewed articles. He graduated 75 theses students at both M.S. and Ph.D. levels in Canada and USA. His research interests include applied electromagnetics, biomedical applications of wireless sensor networks, computer aided design, device modeling, image processing, infrastructure monitoring, neural networks, RF/microwave optimization, unmanned aerial vehicles (UAVs), and virtual reality.

• • •